Air-Water Ring in the Vaneless Gap of a Reversible Pump-Turbine Operating in Condenser Mode

Elena Vagnoni*[1], Loïc Andolfatto[1], Renaud Guillaume[2], Pierre Leroy[2] and François Avellan[1]

[1] EPFL, Laboratory for Hydraulic Machines, Lausanne, Switzerland

[2]GE Renewable Energy, Grenoble, France

Abstract

The present research aims to experimentally study the dynamic characteristics of a rotating bubbly flow in the vaneless gap of a reversible pump-turbine operating in condenser mode by performing high speed image acquisition. Image processing is developed to detect and track the bubbles in the flow for estimating their size and shape and for measuring the velocity profiles. The influence of the gauge pressure is investigated by performing the experiments at five gauge pressure conditions between 2 bar and 17 bar.

The experimental investigation evidences the formation of an air-water ring in the vaneless gap between the impeller blades and the closed guide vanes. The air-water ring is characterized by a rotating bubbly flow due to the air-water mixing. Bubbles have an oblate spheroid shape whose size and velocity depend on the gauge pressure. The velocity is mainly tangential and a periodic fluctuation of both velocity components is recorded owing to the geometrical shape of the guide vanes walls.

Keywords: Two-phase flows; pump-turbine; condenser mode.

Introduction

Hydraulic pump-turbine can be required to operate in condenser mode to compensate the grid instability caused by the penetration of intermittent renewable energy sources [1]. In this particular operating mode, the guide vanes of the pump-turbine are closed and pressurized air is injected in the draft tube cone to reduce the resisting torque by maintaining the water level below the impeller. Furthermore, cooling water is injected through the labyrinth seals.

The sloshing motion of a free surface, turbulent waves causing the formation and entrainment of bubbles diffusing in the water volume and the formation of droplets interfering with the impeller are the main two-phase flow phenomena which have been reported in literature for a turbine operating in condenser mode [2][3][4]. Another expected phenomenon is the onset of an air-water ring in the vaneless gap between the impeller and the closed guide vanes due to the interaction of the water discharge coming from the labyrinth cooling system and water droplets which are generated by the oscillation of the air-water interface. The water droplets entrained by the impeller are expelled from the outer periphery of the impeller by centrifugal force and it forms a rotating air-water ring in the vaneless gap. The rotating flow interacts with the impeller causing power losses. In addition, it is a suitable place for bubble formations and the mass transfer of air into water.

The air-water ring requires further investigations to understand the mechanism of interaction with the impeller and the air mass transfer. To accomplish this goal, the present paper seeks the geometric and dynamic characterization of the rotating air-water ring by performing experimental investigations to estimate the bubbles size and the velocity fields of the flow as a function of the gauge pressure.

Experimental set-up

The experiments are performed on a reduced scale physical model of a high head reversible pump-turbine. A sketch of the main components of the model is illustrated in Figure 1. The model includes the spiral case, 20 guide vanes, 9 blades impeller and the draft tube. The vaneless gap between the impeller and the guide vanes has a ring shape and it measures $0.06 \times D_e$ in height h and $0.09 \times D_e$ in maximum width w, where D_e is the high pressure diameter of the impeller. A generator connected to the impeller regulates the rotational speed. The test rig is operated in closed loop configuration and is equipped with an axial pump which generates the specific hydraulic energy. To operate in condenser mode, the guide vanes are closed and a system of air injection is installed in the draft tube cone. Water is

*Corresponding Author, Elena Vagnoni: elena.vagnoni@epfl.ch

injected through the labyrinth seals for cooling purpose. The Froude similarity is fulfilled by defining the densimetric Froude number as follows:

(1) $$Fr_d = \sqrt{\frac{\rho_a}{\rho_w}} \frac{ND_e}{\sqrt{gD_e}}$$

where N is the rotational speed of the impeller, ρ_a and ρ_w are the air and water density, respectively. The air density is computed from the ideal gas law by measuring the static air pressure in the cone of the draft tube and the temperature. This similarity law has been introduced by Tanaka [2]. The visualization of the water ring in the vaneless gap between the guide vanes and the impeller is performed through two flat optical windows to allow the illumination and the optical access of the vaneless gap and guide vanes as illustrated in Figure 1. The air-water ring visualization is performed with high speed camera, at image acquisition rates of 4'000 frames per second for 8 s. A 95 % uniform LED screen is installed as a back light to enhance the contrast between gaseous and liquid phases.

Tests are performed at five gauge pressure conditions p measured in the cone of the draft tube in air and at $Fr_d = 0.5$. The machines operates in pump rotating direction for all the investigated operating points.

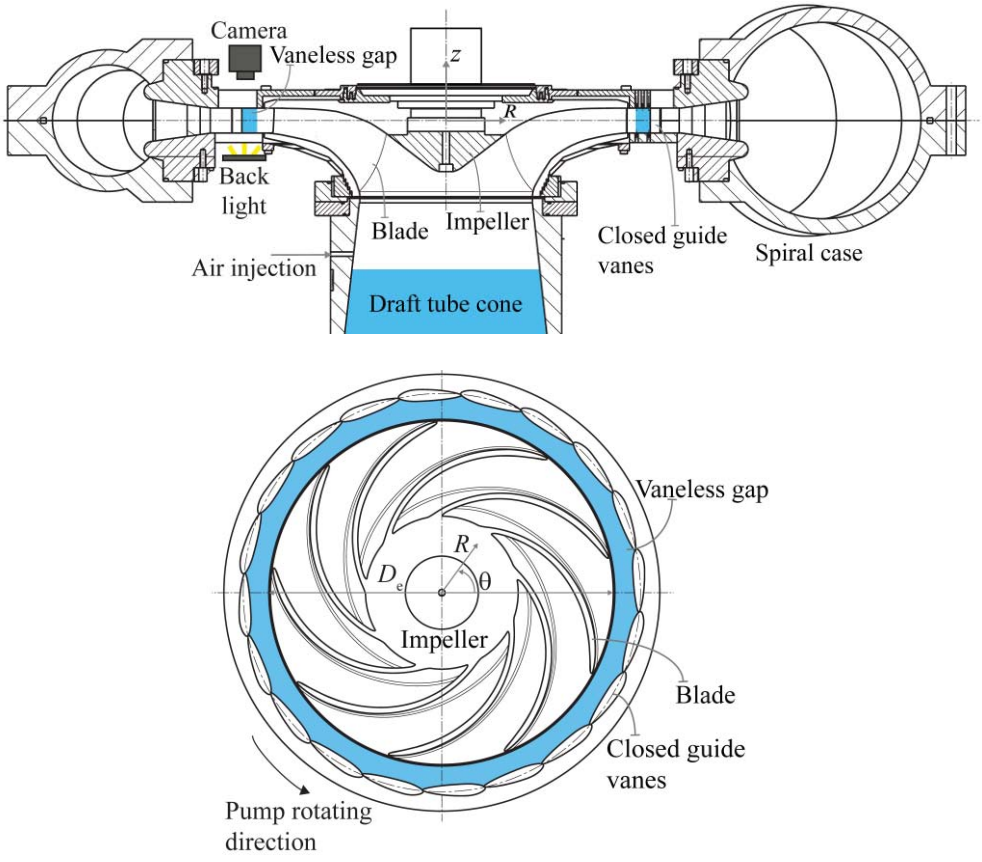

Figure 1. Test facility layout with the instrumentation (right). Top view of the vaneless gap (left).

Image processing method

An image processing method is developed to determine the bubble size and velocity profiles by detecting and tracking the bubbles in the recorded images [5]. As a first step, the images are trimmed to select the region of interest and each pixel of the image is identified by a polar coordinate which corresponds to the polar coordinates system presented in

Figure 1 and Figure 2a). In a second step, the Otsu filter [6] is applied to identify the edge of the bubbles in contrast with the bright background, as shown in Figure 2b). The patterns of interest are the single bubbles represented by the small black areas surrounded by white liquid film. The black areas at the bottom and top of the window correspond to the casing of the machine and they should not be considered as a pattern. Bubbles clusters which cannot be individually distinguished also are discarded. Since the size of one bubble is clearly different on the top and on the bottom black areas and on the clustering of many bubbles, only the features with a perimeter smaller then a fixed value are selected, as illustrated in Figure 2c). On the other side, clusters of few tiny bubbles can be considered as a single feature by the image processing method. In the previous step, each feature is determined by the perimeter, major and minor axis, and the position on the image. The bubbles are assumed to be oblate spheroid with minor semi-axis *a* and major semi-axis *b*. This hypothesis has been validated in literature [7]. For each bubble the equivalent diameter is estimated as follows:

$$d_{eq} = \sqrt[3]{8b^2 a} \tag{2}$$

In the final step, the method links the successive positions of each feature in the following images. The trajectories of the bubbles are identified and the velocity vectors are computed for each bubble as shown in Figure 2d). To compute the radial and angular velocity profiles of both velocity components, the velocities of the bubbles are averaged depending on the bubble position.

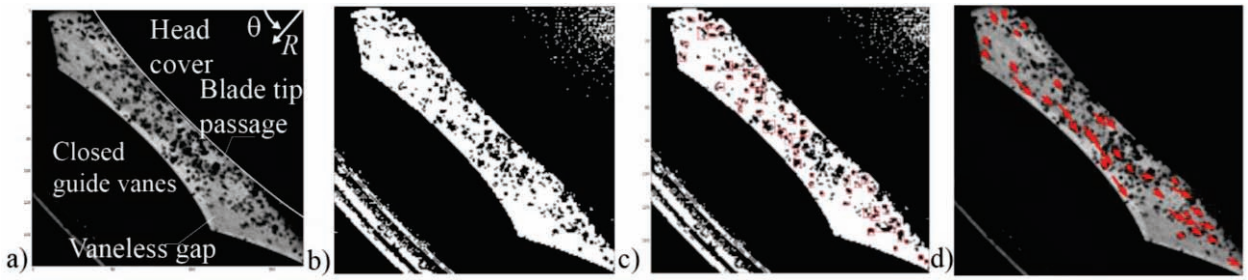

Figure 2. Steps of the image processing method.

Results

Size of bubbles

The high speed visualization enables the observation of the air-water ring in the vaneless gap between the impeller and the guide vanes of a pump-turbine. Images of the air-water ring and the mean equivalent diameter of the bubbles, made non dimensional by dividing for the vaneless gap width *w*, are presented in Figure 3 as a function of the gauge pressure. The boxes extend from the lower to upper quartile values of the data, with a line at the median and a point at the mean value. The whiskers extend from the box to the maximum and minimum values to show the range of the data. It is observed that the boxes and the whiskers extension increases by increasing the gauge pressure. The mean size of the bubbles increases by increasing the gauge pressure and as a consequence, there are more bubbles of different sizes which explains the distribution of the data on a wider range of values.

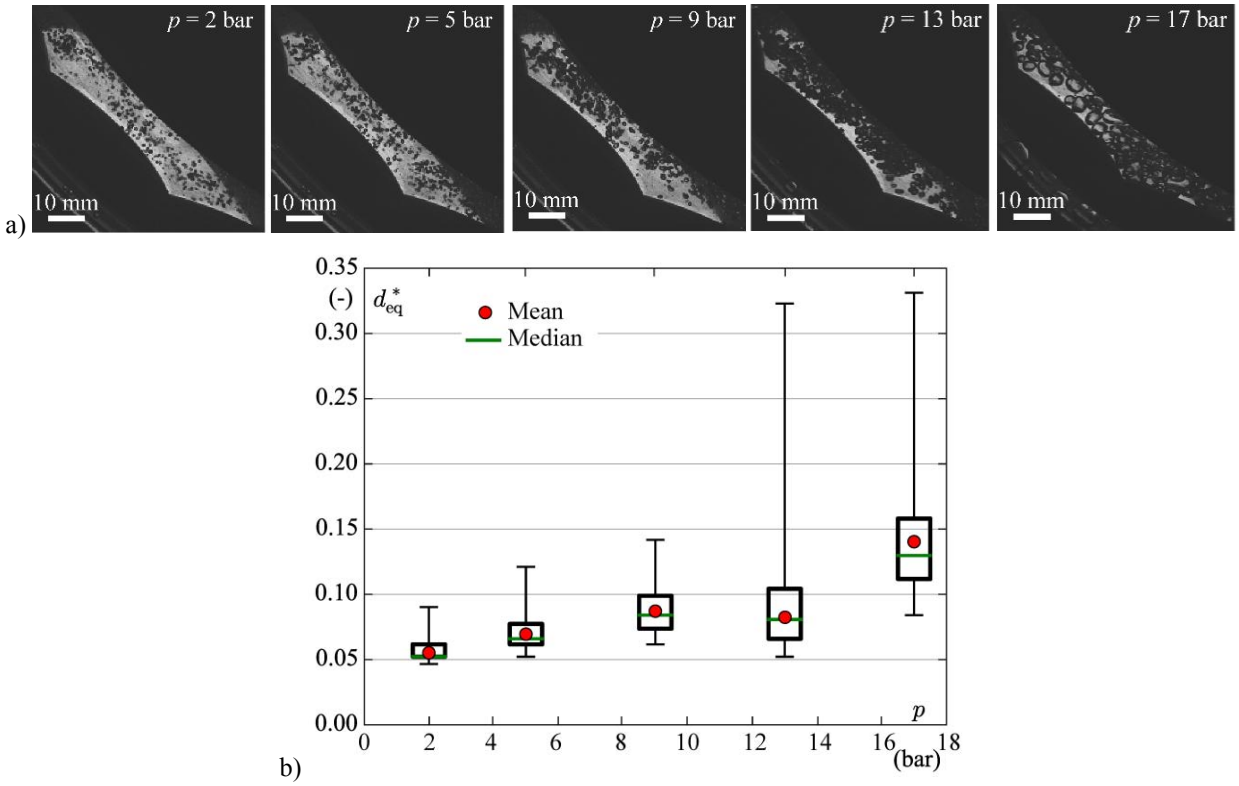

Figure 3. Images of the air water ring (a) and equivalent diameter distribution statistics (b) for the five investigated gauge pressure conditions.

Velocity profiles

The velocity profiles of both tangential and radial components are illustrated in Figure 4. The bubbles velocity is mainly tangential and is slower than the tip of the blades. An influence of the gauge pressure on the tangential velocity divided by the peripheral velocity is recorded. The tangential velocity of the flow at p = 17 bar is lower than the one recorded at the other pressure conditions. This can be explained by the larger size of the bubbles: the formation of clusters of bubbles is observed and they slow down the flow velocity. At p = 13 bar a lower number of bubbles could be tracked due to the higher void fraction. The bubbles at the radius closer to the tip could not be distinguished by the image processing method. Moreover, this introduces a higher standard deviation on both tangential and radial velocity components.

The angular distributions of the tangential and radial velocity components of the bubbles of the air-water ring are presented in Figure 5(a) and (b), respectively at p = 5 bar. The bubbles follow the geometrical shape of the guide vanes by causing a fluctuation of the flow velocity in the vaneless gap which can justify the value of the standard deviation observed in Figure 4 of both velocity components profiles. The tangential velocity decreases in correspondence of the enlargements of the vaneless gap due to the guide vanes shape. The radial velocity component negatively increases in the narrow section of the vaneless gap due to the guide vanes shape and it positively increases in the corresponding enlargement.

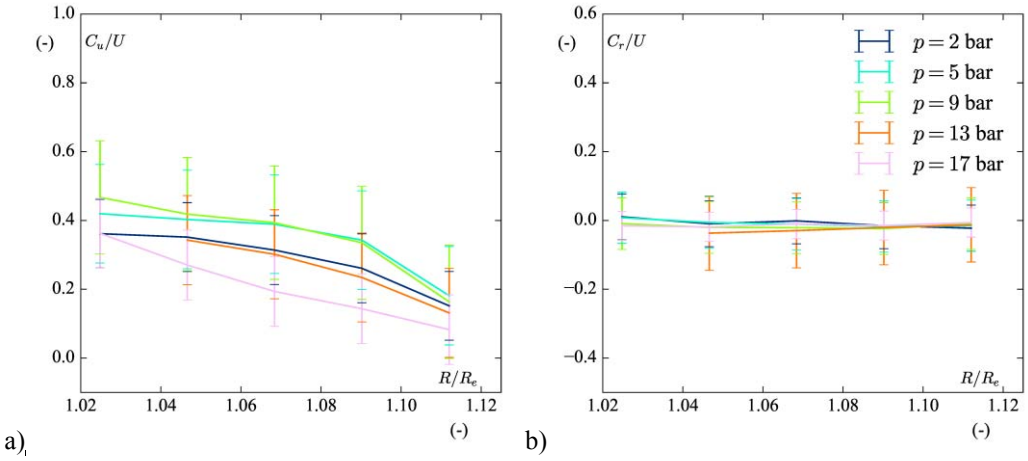

Figure 4. Velocity profile of tangential (a) and radial (b) velocity for the five investigated gauge pressure conditions.

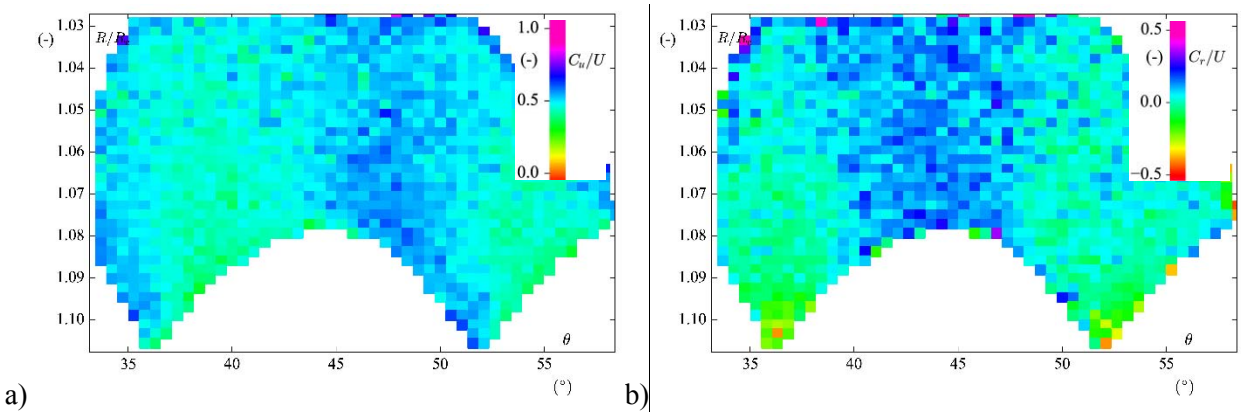

Figure 5. Angular distribution of the tangential (a) and radial (b) velocity components of the bubbles in the air-water ring for p = 5 bar.

Conclusion

In the present work, the dynamic characteristics of the air-water ring in the vaneless gap of a pump-turbine operating in condenser mode are investigated.

High speed visualization and image processing are performed to measure the size and the velocity profiles of the bubbly flow in the air-water ring. Both size and velocity of the bubbles depend on the gauge pressure. The higher the pressure, the larger is the equivalent diameter of the bubbles. At p = 17 bar the size of the bubbles causes the formation of clusters which slow down the velocity of the flow. The measured velocity profiles showed that the flow is mainly tangential in the radial section of the vaneless gap and the fluctuation of both velocity component is due to the geometrical shape of the guide vanes wall.

This study contributes to the understanding of the dynamic characteristics rotating air-water ring in the vaneless gap of a pump-turbine operated in condenser mode. In a further study, we envisage to estimate the parameters of the mass transfer of air in water to compute the air losses through the vaneless gap.

Acknowledgements

The research leading to the results published in this paper has received funding from GE Renewable Energy France. The authors would like to thank the team of GE Renewable Energy France for their collaboration and technical support, in particular Yann Viguen Heratchian and Pierre-Yves Lowys.

References

[1] I. Rychkov, *Reactive power control services based on a generator operating as a synchronous condenser*, Power Technology and Engineering 46, pp. 405-409, (2013).

[2] H. Tanaka, K. Matsumoto, K. Yamamoto, *Sloshing motion of the depressed water in the draft tube in dewatered operation of high head pump-turbines*, XVII IAHR Symposium on hydraulic machines and cavitation, Beijing, Chine (1994).

[3] Rossi, G. and Zanetti, V., *Starting in air and synchronous condenser operation of pump-turbines - Model research*, 9th IAHR-SHMEC Symposium, vol. 2, pp. 337-352,Fort Collins (USA), (1978).

[4] O. Ceravola, M. Fanelli, B. Lazzaro, *The behavior of the free level below the impeller of Francis turbines and pump-turbine in operation as synchronous condenser*, Proceedings of X IAHR Symposium on hydraulic machines and cavitation, Tokyo, Japan 1 (1980) 765-775.

[5] S. van der Walt, J. Schonberger, J. Nunez-Iglesias, F. Boulogne, J. Warner, N. Yager, E. Gouillart, T. Yu, *scikit-image: image processing in python*, 350 PeerJ 2:e453 doi:https://doi.org/10.7717/peerj.453.

[6] R. Gonzales, R. Woods, *Digital image processing*, Pearson Education International, 2008.

[7] D. Colombet, D. Legendre, A. Cockx, P. Guiraudand, F. Risso, C. Daniel, S. Galinat, *Experimental study of mass transfer in a dense bubble swarm*, Chemical Engineering Science 66 (2011) 3432-3440.

© 2018 ASME